Optimizing Foot Centers of Pressure through Force Distribution in a Humanoid Robot

Patrick M. Wensing, Ghassan Bin Hammam,
Behzad Dariush, and David E. Orin

June 5, 2013

Abstract

The force distribution problem (FDP) in robotics requires the determination of multiple contact forces to match a desired net contact wrench. For the double support case encountered in humanoids, this problem is underspecified, and provides the opportunity to optimize desired foot centers of pressure (CoPs) and forces. In different contexts, we may seek CoPs and contact forces that optimize actuator effort or decrease the tendency for foot roll. In this work, we present two formulations of the FDP for humanoids in double support, and propose objective functions within a general framework to address the variety of competing requirements for the realization of balance. As a key feature, the framework is capable to optimize contact forces for motions on uneven terrain. Solutions for the formulations developed are obtained with a commercial nonlinear optimization package and through analytical approaches on a simplified problem. Results are shown for a highly dynamic whole-body humanoid reaching motion performed on even terrain and on a ramp. A convex formulation of the FDP provides real-time solutions with computation times of a few milliseconds. While the convex formulation does not include CoPs explicitly as optimization variables, a novel objective function is developed which penalizes foot CoP solutions that approach the foot boundaries.

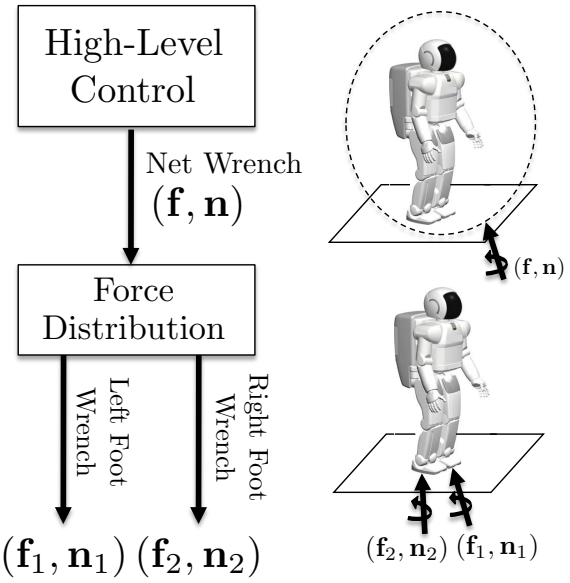

Figure 1: Force distribution block diagram and setting. The general approach taken in this work resolves a required net wrench (with force $\mathbf{f}$ and moment $\mathbf{n}$) on the system to two foot wrenches in an optimal manner.

1 Introduction

The force distribution problem (FDP) in robotics is a fundamental problem that requires the computation of physically feasible contact forces to match a desired net contact wrench. Solutions to this problem have been studied to properly select foot forces in multilegged robots, with early formulations appearing decades ago.[1–4] Point contacts at the feet, which can generate no moments, are typically assumed to simplify the problem. The FDP for humanoid robots, described by Fig. 1, does not permit this assumption and requires a more general distribution of the wrench to each foot, due to planar contacts which can generate significant moments. Although this complexity introduces additional constraints on the individual foot wrenches, the FDP is generally underspecified and provides the opportunity to optimize the foot centers of pressure (CoPs) and contact forces. The study here addresses how to efficiently formulate the FDP for humanoids and to optimally select foot CoPs and forces for minimum actuator effort and to prevent foot roll.

The FDP formulation presented here is general to any humanoid model. The desired *net* wrench input to the FDP in Fig. 1, however, will often be based on a specific whole-body dynamic model and may come from any number of high-level controllers. For instance, the net wrench may be specified from some desired pre-computed dynamics,[5] from the intermediate product of a whole-body control strategy,[6] or from desired center of mass (or more generally, centroidal[7]) dynamics.[8,9] In the latter case, the desired net contact wrench is precisely determined by the desired rate of change in the net system linear and angular momentum. Once the FDP is solved, methods to physically realize the optimized ground reaction forces and CoPs will be dependent on the dynamic and kinematic parameters of the model. Still, as it will be shown, the FDP itself relies purely on the kinematic parameters of the humanoid and contact limitations such as friction. Examples of how force distribution fits within the context of whole-body control are given in Section 2 and in previous work.[6]

In this paper, we focus on the case of force distribution for a humanoid robot in double support. Preliminary force distribution algorithms[10–12] have been required in many of the most advanced force-controlled humanoids, and will continue to be one of several algorithms needed for humanoids to operate compliantly within a force-controlled framework. In single support, the force distribution problem is trivial; every feasible net contact wrench implies a unique foot CoP and required ground reaction force (GRF). Yet, in double support, there are numerous ways to resolve the net contact wrench into two foot CoPs and GRFs. While much legged robotics research has concentrated on the control of periodic motions dominated by single support (e.g.[13]), many useful humanoid tasks such as lifting[14] or household cleaning[15] occur predominantly in double

support. Double support force distribution algorithms will also be necessary for force-controlled humanoids to perform human motion transfer and retargeting tasks,[6] walking gaits with extended periods of double support,[16] or any other motion that requires intermittent steps. Algorithms to compute force distributions for more complex contact scenarios are a straightforward extension once contact force optimization has been addressed through study of double support.

1.1 Related Work

In double support, a net wrench's distribution to each foot is generally underspecified. While this contact force underspecification has been addressed in-part in the force-controlled humanoids community, the opportunity to *optimize* these contact forces and CoPs for a variety of objectives pertinent to dynamic balance has yet to be fully explored. Preliminary studies have been dominated by pseudo-inverse based approaches and constrained optimization approaches.

Pseudo-inverse approaches have been used to address contact force underspecification by a number of researchers, but limit the potential objectives and do not enforce frictional constraints on the GRFs. Mistry, et al.[5] and Righetti et al.[10] addressed contact force underspecification for floating-base inverse dynamics (ID). Due to ground contacts, the ID problem does not have a unique solution in double support. Their approach decomposes the system dynamics and uses pseudo-inverse methods to provide force distributions which optimize joint torque norms[5] or quadratic objectives of the contact forces.[10] More complex objectives, such as those on CoP studied here, have not been shown to be compatible with their framework.

Hyon et al.[11] solve the force distribution problem for compliant multi-contact behaviors. Their pseudo-inverse solution considers the optimization of contact force norms, but again does not enforce friction limits on the GRFs. While this drawback was partially addressed with an impedance based control law,[8] the approach, by construction, allows some foot slip. Friction constraints are included here which provides a strong guarantee on the physical realizability of the contact forces that emerge from our FDP solutions.

Sentis et al.[15] partially address force underspecification within their prioritized multi-tasking framework.[17] The last level in their prioritized control framework selects torques which modify the force distribution, but do not disturb the desired dynamics dictated from the higher-priority control levels[1]. As opposed to optimizing contact forces, their objective is to produce no moments at desired contact CoPs as well as to achieve certain interaction forces and moments between the contacts. Due to their pseudo-inverse based approach, feasible contact forces do not always result (even when they may exist to realize the desired dynamics), and it is necessary to check friction constraints in an additional step. Through the use of constrained optimization, the FDP formulation for planar contact introduced here guarantees that feasible contact forces will result, when they exist, to match the required wrench.

Others have formulated the force distribution problem more formally as a constrained optimization problem and have employed sub-optimal solution methods or used various simplifying assumptions. Sub-optimal force distribution was presented in[6] for the case of a side by side stance. Efficient algorithms to test feasibility of the force distribution problem were used to produce non-optimized contact forces.[19] More general solutions have emerged recently by Stephens and Atkeson[12] and Lee and Goswami.[9] Both approaches use a linear approximation to the friction cone constraints and consider a single objective. Stephens and Atkeson optimize the ground force magnitudes (similar to[8]), yet enforce friction constraints more satisfactorily. While only considering this simple objective, they demonstrate the usefulness of the force distribution problem to lifting tasks as well as postural maintenance. Lee and Goswami optimize ankle torques and apply a multi-stage optimization process that results in near-optimal solutions. In contrast, we use general convex optimization to show how friction cone constraints can be enforced and how CoP-based objectives can be optimized in real time.

The remainder of this paper is organized as follows. Section 2 introduces the FDP within the context of floating-base inverse dynamics. Sections 3 and 4 then provide and contrast two formulations of the FDP for planar contacts. These formulations differ in the manner through which each foot wrench is characterized. The section following provides a description of the direct applicability of the force distribution algorithm to uneven terrain and gives results for motion on a ramp. Section 6 presents a new objective to avoid foot roll through a novel optimization of foot CoP margins that is able to be computed in real time. Finally, the work is summarized and conclusions of the work are discussed.

[1]Thus, this final layer of control essentially solves a floating-base ID problem. This connection has been formalized.[18]

2 Background

While the FDP has been recognized within the multilegged robotics community for quite some time, it is a relatively new area of study for application to humanoid robots. To assist in its introduction, this section will demonstrate an example application of the FDP to solve floating-base inverse dynamics in double support. Let the generalized coordinates for a floating-base humanoid be decomposed as $\mathbf{q} = [\mathbf{q}_u^T, \mathbf{q}_a^T]^T$ where $\mathbf{q}_u \in \mathbb{R}^6$ and $\mathbf{q}_a \in \mathbb{R}^n$ are the unactuated (floating-base) and actuated degrees of freedom (DOFs) respectively. Consider the standard equations of motion for a floating-base humanoid:[20]

$$\mathbf{H}\ddot{\mathbf{q}} + \mathbf{C}\dot{\mathbf{q}} + \mathbf{G} = \mathbf{J}_c^T \mathbf{f}_c + \mathbf{S}_a^T \boldsymbol{\tau}_a \tag{1}$$

where $\mathbf{H}$, $\mathbf{C}\dot{\mathbf{q}}$, and $\mathbf{G}$ are the familiar mass matrix, velocity product terms, and gravitational terms respectively. Following the conventions of Fig. 1, we define the combined contact force $\mathbf{f}_c = [\mathbf{n}_1^T, \mathbf{f}_1^T, \mathbf{n}_2^T, \mathbf{f}_2^T]^T$. Here $\mathbf{J}_c = [\mathbf{J}_1^T \ \mathbf{J}_2^T]^T$ is a combined contact Jacobian for the feet, $\boldsymbol{\tau}_a \in \mathbb{R}^n$ is the vector of actuated joint torques, and $\mathbf{S}_a = [\mathbf{0}_{n\times 6} \ \mathbf{I}_{n\times n}]$ is a selection matrix which encodes the system's actuation. Similarly, we define $\mathbf{S}_u = [\mathbf{I}_{6\times 6} \ \mathbf{0}_{6\times n}]$. The floating-base ID problem is as follows: given a robot state $(\mathbf{q}, \dot{\mathbf{q}})$ and some desired accelerations $\ddot{\mathbf{q}}_d$, select $\boldsymbol{\tau}_a$ to achieve $\ddot{\mathbf{q}}_d$. It is assumed that the robot state and $\ddot{\mathbf{q}}_d$ are consistent with double support. Standard open-chain ID[20] can be used to compute the quantity:

$$\tilde{\boldsymbol{\tau}} = \mathbf{H}\ddot{\mathbf{q}}_d + \mathbf{C}\dot{\mathbf{q}} + \mathbf{G} \ .$$

In order to achieve $\ddot{\mathbf{q}}_d$, we then have the following system of equations in $\boldsymbol{\tau}_a$ and $\mathbf{f}_c$:

$$\mathbf{S}_u\tilde{\boldsymbol{\tau}} = \mathbf{S}_u\mathbf{J}_c^T\mathbf{f}_c = \mathbf{S}_u\left(\mathbf{J}_1^T \begin{bmatrix} \mathbf{n}_1 \\ \mathbf{f}_1 \end{bmatrix} + \mathbf{J}_2^T \begin{bmatrix} \mathbf{n}_2 \\ \mathbf{f}_2 \end{bmatrix}\right) \tag{2}$$

$$\mathbf{S}_a\tilde{\boldsymbol{\tau}} = \mathbf{S}_a\mathbf{J}_c^T\mathbf{f}_c + \boldsymbol{\tau}_a \ . \tag{3}$$

Here, (2) states that the floating-base wrench $\mathbf{S}_u\tilde{\boldsymbol{\tau}}$ found from open-chain ID must be equal to the sum of the left and right foot wrenches (expressed at the floating base). As a result, the left side of (2) represents the net wrench that should be input to the force distribution problem for this application. Note that (2) is a system of 6 equations, with 12 unknown components of $\mathbf{f}_c$ to be selected. As a result, this equation is underspecified in $\mathbf{f}_c$ and thus allows flexibility in the distribution of the net wrench to each foot. Once the FDP is solved, with the optimal contact wrenches denoted as $\mathbf{f}_c^*$, (3) can be rearranged as

$$\boldsymbol{\tau}_a = \mathbf{S}_a\left(\tilde{\boldsymbol{\tau}} - \mathbf{J}_c^T\mathbf{f}_c^*\right)$$

which specifies the joint torques required to achieve $\ddot{\mathbf{q}}_d$ and to physically realize $\mathbf{f}_c^*$. While model-specific mass and inertia parameters were required for the computation of $\tilde{\boldsymbol{\tau}}$, it will be shown that the FDP formulation relies only on the geometric parameters of the contacts and their friction limitations. In this paper we demonstrate how to optimize the foot wrenches and associated CoPs subject to wrench balance constraints similar to (2), as well as other constraints of physical realizability. The next sections study how to efficiently represent $\mathbf{f}_c$ for optimization.

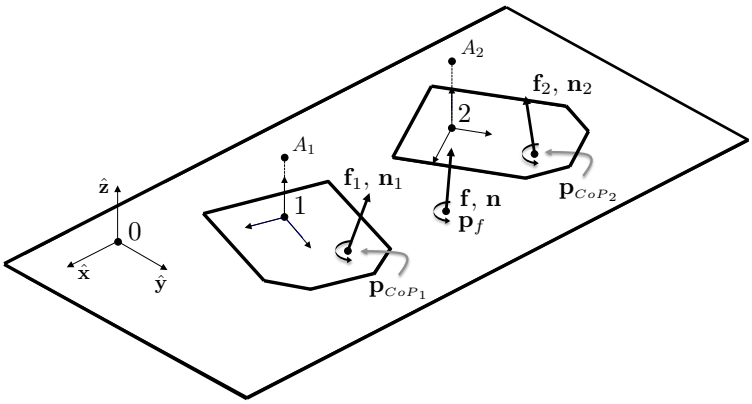

Figure 2: Coordinate system and variable description for the Foot CoPs formulation.

3 Foot CoPs Optimization Formulation

In the first formulation of the force distribution problem (FDP), the net wrench *for each foot* will be characterized by its center of pressure (CoP) and a wrench which acts at this CoP. In this manner, on even terrain, the force distribution can be thought of as the distribution of a global ZMP (and associated wrench) to two local CoPs (and associated wrenches). It is assumed that each foot is in contact with the ground through a planar convex polygonal contact. Figure 2 illustrates these contact conditions for the case when all ground supports are co-planar. Note that the formulation as developed below is based on a net wrench (not ZMP) and thus may be applied to uneven terrain without any changes to the formulation.

Figure 2 provides a graphical description of the given variables for this formulation. Each FDP requires the realization of a required wrench given by a force and moment $(\mathbf{f}, \mathbf{n})$ which acts at a position $\mathbf{p}_f$. Expressed in the global coordinate system, these vectors are represented by the quantities ${}^0\mathbf{f}$, ${}^0\mathbf{n}$, and ${}^0\mathbf{p}_f$ respectively. The position and orientation of foot i is given by the pair $({}^0\mathbf{p}_i, {}^0\mathbf{R}_i)$ where ${}^0\mathbf{R}_i \in \mathbb{R}^{3\times 3}$ is the rotation matrix for foot i. Each local coordinate frame is defined such that the $z = 0$ plane contains the local plane of contact, and thus its $\hat{\mathbf{z}}$ axis is normal to this plane. Additionally, each foot has an associated ankle center A_i, with position in local coordinates given by ${}^i\mathbf{p}_{A_i}$.

The optimization variables for foot i prescribe a local center of pressure ${}^i\mathbf{p}_{CoP_i}$ and associated wrench $\left({}^i\mathbf{f}_i, {}^i\mathbf{n}_i\right)$. Due to the local coordinate system conventions outlined previously, these optimization variables take the form:

$$ {}^i\mathbf{p}_{CoP_i} = [{}^i p^x_{CoP_i}, {}^i p^y_{CoP_i}, 0]^T, \quad {}^i\mathbf{n}_i = [0, 0, {}^i n^z_i]^T, \tag{4} $$

where the leading superscript i indicates that the components are given in the coordinate frame attached to foot i. This section will introduce the constraints and objectives considered for this formulation. A simplification of the Foot CoPs formulation will then be presented and solved in order to extract the approximate behavior of the full formulation for many contact cases.

3.1 Force and Moment Balance Constraints

For the force distribution to be valid, the net effect of the foot wrenches must be statically equivalent to the desired wrench. This leads to the following constraints:

$$ {}^0\mathbf{f} = \sum_{i=1}^{2} {}^0\mathbf{R}_i \, {}^i\mathbf{f}_i \tag{5} $$

$$ {}^0\mathbf{n} = \sum_{i=1}^{2} {}^0\mathbf{R}_i \left[{}^i\mathbf{n}_i + \left({}^i\mathbf{p}_{CoP_i} - {}^i\mathbf{p}_f \right) \times {}^i\mathbf{f}_i \right] . \tag{6} $$

While the force balance constraint in (5) is *linear*, the three equations from the moment balance constraint in (6) are *nonlinear* in the optimization variables. This nonlinearity arises due to the position-force cross

terms, ${}^i\mathbf{p}_{CoP_i} \times {}^i\mathbf{f}_i$, that appear in the constraint. Thus, this constraint introduces non-convexity into this formulation.

3.2 Friction Constraints

To prevent foot slip, the wrench at each foot CoP must obey constraints given by:

$$\sqrt{({}^i f_i^x)^2 + ({}^i f_i^y)^2} \leq \mu_{f_i} {}^i f_i^z \tag{7}$$

$$|{}^i n_i^z| \leq \mu_{n_i} {}^i f_i^z \tag{8}$$

where μ_{f_i} is the static coefficient of friction and μ_{n_i} is a torsional friction coefficient[21] which provides an approximation that is dependent upon the contact surface conditions. Constraint (7) is a second-order cone constraint (it is nonlinear, but still convex) and is easily handled by many computational optimization methods.[22] The *friction cone* for each foot will be denoted as:

$$\mathcal{K}_i = \left\{ \mathbf{f} \in \mathbb{R}^3 \;\middle|\; \sqrt{(f^x)^2 + (f^y)^2} \leq \mu_{f_i} f^z \right\}. \tag{9}$$

In addition to a constraint on the magnitude of the tangential force at each CoP, these friction constraints restrict the normal force to be non-negative.

3.3 Center of Pressure Constraints

Finally, for each of the CoPs to be physically realizable, they must reside within the contact polygon of the foot. From the assumption that each foot is in convex polygonal contact with the ground, this can be expanded as a set of linear inequality constraints:

$$\mathbf{B}_i \begin{bmatrix} {}^i p_{CoP_i}^x \\ {}^i p_{CoP_i}^y \end{bmatrix} \leq \mathbf{c}_i \tag{10}$$

for some $\mathbf{B}_i \in \mathbb{R}^{m_i \times 2}$ and $\mathbf{c}_i \in \mathbb{R}^{m_i}$, where m_i is the number of sides for the polygonal contact on foot i. For later convenience we define $\mathcal{F}_i$ as the set of all CoP locations which satisfy this constraint

3.4 Initial Objective Function

The first objective considered is to properly select foot CoP locations and associated forces in order to minimize the required ankle effort. Proper CoP selection for this objective is pertinent in many applications to find energy-efficient solutions and to minimize the performance requirements on the ankle actuators. Minimizing this requirement is particularly important since the ankle, as the distal joint, often employs the smallest and lowest power actuators. A similar goal is also considered by Lee and Goswami[9] to minimize the possibility for foot roll. This objective is motivated from a biomimetic standpoint as well, as biomechanics studies have shown that minimal ankle torques are employed for dynamic balance in order to maintain full foot contact with the environment.[23] To formalize this objective, the sum of squared ankle torque is minimized as:

$$\min \sum_{i=1}^{2} \| \left({}^i\mathbf{p}_{CoP_i} - {}^i\mathbf{p}_{A_i} \right) \times {}^i\mathbf{f}_i + {}^i\mathbf{n}_i \|^2 . \tag{11}$$

Once again, the position-force cross terms lead to undesirable characteristics for this formulation, as this objective is non-convex. The full Foot CoPs FDP can now be formulated and is given by:

$$\begin{aligned} \min \;& \sum_i \|({}^i\mathbf{p}_{CoP_i} - {}^i\mathbf{p}_{A_i}) \times {}^i\mathbf{f}_i + {}^i\mathbf{n}_i\|^2 \\ \text{s.t. } & (5), (6) \\ & (7),\ (8),\ (10), {}^i p_{CoP_i}^z = 0 \quad \forall i \in \{1, 2\} \end{aligned}$$

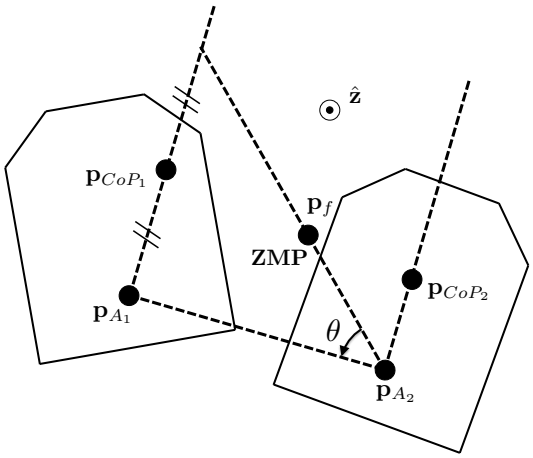

Figure 3: Graphical description of the optimal CoP location for the Foot CoPs formulation with simplifying assumptions.

3.5 Simplifying Assumptions

For many motions, the required wrench will be dominated by a gravity compensation force. Thus, to provide a sub-optimal solution of the Foot CoPs formulation on flat terrain the following simplifications will be considered:

- It is assumed that the desired wrench has been transformed to a desired ZMP on a level ground plane of contact. Thus ${}^0\mathbf{p}_f = [{}^0p_f^x, {}^0p_f^y, 0]^T$. This can be accomplished with standard ZMP calculations as provided elsewhere.[24]
- It is assumed that the net wrench expressed at the ZMP has negligible tangential force and normal moment. That is, ${}^0\mathbf{f} = [0, 0, {}^0f^z]^T$ and ${}^0\mathbf{n} = \mathbf{0}$.
- The desired wrench will be matched through distribution of the normal force only. That is, ${}^0\mathbf{f}_i = [0, 0, {}^0f_i^z]$. As a result, the ankle height has no bearing on the objective (11) so we select ${}^0\mathbf{p}_{A_i} = [{}^0p_{A_i}^x, {}^0p_{A_i}^y, 0]^T$.
- All variables are expressed in global coordinates.

Under these simplifications, and disregarding the unidirectional force and foot boundary constraints for the time being, a unique local optima exists and employs a left foot CoP position given by:

$$\mathbf{p}_{CoP_1/A_1} = \frac{\mathbf{p}_{A_1/A_2} \tan(\theta) \times \hat{\mathbf{z}}}{2} \tag{12}$$

where the notation $\mathbf{p}_{a/b}$ represents the vector $\mathbf{p}_a - \mathbf{p}_b$ and θ is the angle about the $\hat{\mathbf{z}}$ axis from $\mathbf{p}_{f/A_2}$ to $\mathbf{p}_{A_1/A_2}$. This optimal CoP is shown graphically in Fig. 3. This result can be found through analysis of the first-order necessary conditions for equality-constrained local minima with the assumptions described previously. The main result here is that *the optimal centers of pressure lie along the lines perpendicular to the line between the ankle centers.* Also, the optimal CoPs are required to be co-linear with the ZMP to satisfy the moment balance constraints. Further, as long as $\mathbf{p}_f$ lies within the perpendicular lines at the ankle centers, the corresponding optimal foot forces satisfy $f_i^z \geq 0$. Thus, if this condition on $\mathbf{p}_f$ holds and the optimal CoPs are within the foot boundaries, then this geometric solution is the global optimum for the FPD under the assumptions described. We compare the optimum of the simplified problem to that of the general formulation through numerical optimization in the next sections.

3.6 Numerical Optimization

To determine the (non-simplified) Foot CoP formulation's applicability for use in real-time control, a solution method was developed with the KNITRO optimization package in C++.[25] This optimization package

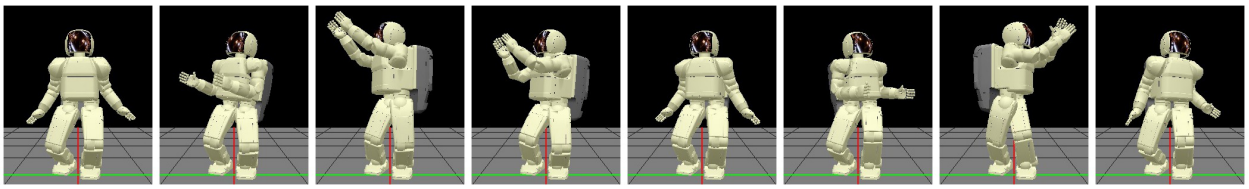

Figure 4: Motion snapshots from a 5.4s section of the CMU reaching motion.[26] This motion was used to assess the real-time performance of the force distribution algorithm.

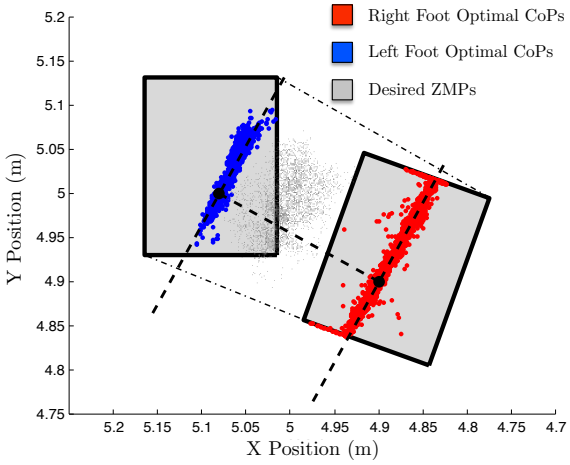

Figure 5: Optimal CoPs as found by the Foot CoPs formulation for the CMU reaching motion.[26]

provides algorithms to solve general nonlinear programming problems and thus is applicable for use with the full non-convex Foot CoPs formulation presented earlier. The package contains both active-set and non-traditional interior-point algorithms. To aid the iterative algorithms in the KNITRO package, analytic gradients and Hessians for the objective and constraints were provided to the optimization routines in this work.

3.7 Results

To assess the real-time performance of the Foot CoPs formulation, the optimization algorithm was tested on a reaching motion from the CMU motion library.[26] This motion is highly dynamic[6] in comparison to motions performed by state-of-the-art humanoid robots. With methods developed previously,[6] this motion was kinematically and dynamically retargeted to a model of Honda's humanoid and is shown in Fig. 4. The motion is 45.8s in length and we seek to solve the FDP every 10 ms (4580 total instances of the FDP). Model-specific methods described in Section 2 were used to extract the required net wrench at each of the 4580 instants of motion.

The optimal foot CoPs found by the force distribution algorithm are shown in Fig. 5. On a MacBook Pro with a 2.26GHz Intel Core 2 Duo processor, the force distribution algorithm required 73.2 ms to reach a solution on average and over 600 ms in the worst case. While the optimal foot CoPs in the non-simplified case do not fall exactly on the lines perpendicular to the line between the ankle centers, this behavior is generally observed. Thus, while this formulation is not suitable for real-time control, *the simplified solution can often be used to obtain a fast and satisfactory solution to the FDP*. This sub-optimal approach is often adequate for locomotion on level surfaces.

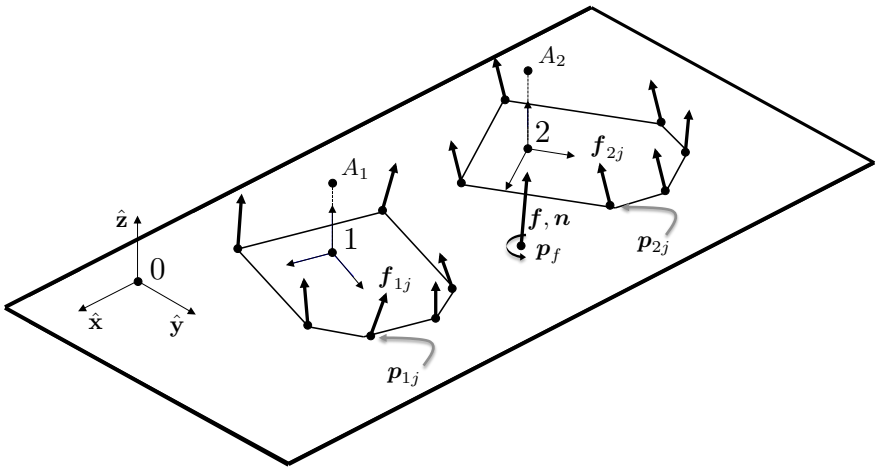

Figure 6: Coordinate system and variable description for the Contact Vertices formulation. Note that the definition of the optimization variables is general to uneven terrain cases.

4 Contact Vertices Formulation

This section will describe another formulation of the FDP that enables solutions in real time for a general setting. In the previous formulation, non-convexities were present due to position-force cross terms that appeared in the objective function and moment balance constraint. To eliminate this drawback, instead of optimizing foot CoP locations directly, a formulation will be proposed that considers a lattice of contact points that are *instantaneously fixed* for each instance of the FDP. CoP objectives can still be optimized with new approaches described in Section 6.

In this formulation, each foot wrench will be approximately represented by a set of forces which act at the contact polygon vertices. Figure 6 provides a graphical description of the quantities, $\mathbf{p}_{ij}$ and $\mathbf{f}_{ij}$, where $\mathbf{p}_{ij}$ is contact vertex j for foot i, and $\mathbf{f}_{ij}$ is the force acting at contact vertex j for foot i where $i \in \{1, 2\}$ and $j \in \{1, 2, ..., m_i\}$ and m_i is the number of vertices for foot i. While any lattice of contact points underneath each foot may be selected, this particular contact discretization is employed in other humanoid work.[11,19,27] The full contact force optimization vector $\mathbf{f}_c$ is then redefined as:

$$\mathbf{f}_c = [{}^1\mathbf{f}_{11}^T, \ldots, {}^1\mathbf{f}_{1\,m_1}^T, {}^2\mathbf{f}_{21}^T, \ldots, {}^2\mathbf{f}_{2\,m_2}^T]^T \,.$$

4.1 Force and Moment Balance Constraints

Again, the distribution of force must be statically equivalent to the desired wrench:

$${}^0\mathbf{f} = \sum_{i=1}^{2}\sum_{j=1}^{m_i} {}^0\mathbf{R}_i \, {}^i\mathbf{f}_{ij} \,, \text{ and} \tag{13}$$

$${}^0\mathbf{n} = \sum_{i=1}^{2}\sum_{j=1}^{m_i} {}^0\mathbf{R}_i \left[({}^i\mathbf{p}_{ij} - {}^i\mathbf{p}_f) \times {}^i\mathbf{f}_{ij}\right] = \sum_{i=1}^{2}\sum_{j=1}^{m_i} {}^0\mathbf{R}_i \mathbf{S}({}^i\mathbf{p}_{ij} - {}^i\mathbf{p}_f) {}^i\mathbf{f}_{ij} \,, \tag{14}$$

where $\mathbf{S}(\mathbf{p})$ is the skew-symmetric cross product matrix :

$$\mathbf{S}(\mathbf{p}) = \begin{bmatrix} 0 & -p_3 & p_2 \\ p_3 & 0 & -p_1 \\ -p_2 & p_1 & 0 \end{bmatrix} \tag{15}$$

for $\mathbf{p} = [p_1, p_2, p_3]^T$ which provides $\mathbf{S}(\mathbf{p})\mathbf{r} = \mathbf{p} \times \mathbf{r}$, $\forall\, \mathbf{r} \in \mathbb{R}^3$. The matrices $\mathbf{S}({}^i\mathbf{p}_{ij} - {}^i\mathbf{p}_f)$ are known and constant for each instance of the FDP. Thus, both the force and moment balance constraints here are linear

	Foot CoPs Form.	**CV Form.**
Objective	Non-Convex	Convex (Quadratic)
Variables	12	$3m$
Linear Ineq. Constr.	$4+m$	0
Nonlinear Ineq. Constr.	2	m
Linear Eq. Constr.	3	6
Nonlinear Eq. Constr.	3	0
Average Comp. Time	73.2 ms	1.75 ms
Worse Case Comp. Time	620 ms	10.8 ms

Table 1: Formulation comparison. Computational times were measured on a MacBook Pro with a 2.26GHz Intel Core 2 Duo processor.

constraints. For compactness we will express the desired net external wrench as ${}^0\mathbf{w} = [{}^0\mathbf{n}^T, {}^0\mathbf{f}^T]^T$. Letting $m = m_1 + m_2$, we combine the force and moment balance equations as:

$$ {}^0\mathbf{w} = \mathbf{A}\mathbf{f}_c \tag{16}$$

where $\mathbf{A} \in \mathbb{R}^{6\times 3m}$.

4.2 Friction Constraints

Once again, a coulomb friction model is adopted at each contact. We retain the friction cone definition provided previously and require:

$$ {}^i\mathbf{f}_{ij} \in \mathcal{K}_i \quad \forall i \in \{1,2\}, j \in \{1,2,\ldots,m_i\}\,. $$

Succinctly, this constraint is written as $\mathbf{f}_c \in \mathcal{K}_c$.

4.3 Initial Objective Function

Once again, the minimization of ankle effort is considered. The fixed nature of the contact points allows the position-force cross product to be expressed as a constant matrix multiplication with the optimization variables.

$$ \min \sum_{i=1}^{2} \left\| \left[\sum_{j=1}^{m_i} \mathbf{S}\left({}^i\mathbf{p}_{ij} - {}^i\mathbf{p}_{A_i}\right) {}^i\mathbf{f}_{ij} \right] \right\|^2 = \min \sum_{i=1}^{2} \mathbf{f}_{c_i}^T \mathbf{Q}_i^T \mathbf{Q}_i \mathbf{f}_{c_i} = \min \mathbf{f}_c^T \mathbf{Q}\, \mathbf{f}_c \tag{17}$$

where

$$ \mathbf{Q}_i = [\mathbf{S}({}^i\mathbf{p}_{i1} - {}^i\mathbf{p}_{A_i}), \ldots, \mathbf{S}({}^i\mathbf{p}_{i\,m_i} - {}^i\mathbf{p}_{A_i})] \quad \text{and} \quad \mathbf{Q} = \mathrm{diag}(\mathbf{Q}_1^T\mathbf{Q}_1, \mathbf{Q}_2^T\mathbf{Q}_2). $$

The Contact Vertices formulation does not suffer from the non-convexities found in the Foot CoPs formulation. The objective is a positive semi-definite quadratic form of the optimization vector and thus is convex. The full Contact Vertices formulation can now be fully written in compact form and is given by:

$$ \begin{aligned} &\min \mathbf{f}_c^T \mathbf{Q}\, \mathbf{f}_c \\ &\text{s.t. } {}^0\mathbf{w} = \mathbf{A}\mathbf{f}_c \\ &\quad \mathbf{f}_c \in \mathcal{K}_c\,. \end{aligned} \tag{18}$$

This formulation is similar in spirit to FDPs found in point-contact force optimization.[28] Still, the use of this framework will not prevent the development of explicit CoP objectives that are specific to planar contacts. These additional objectives will be developed in Section 6.

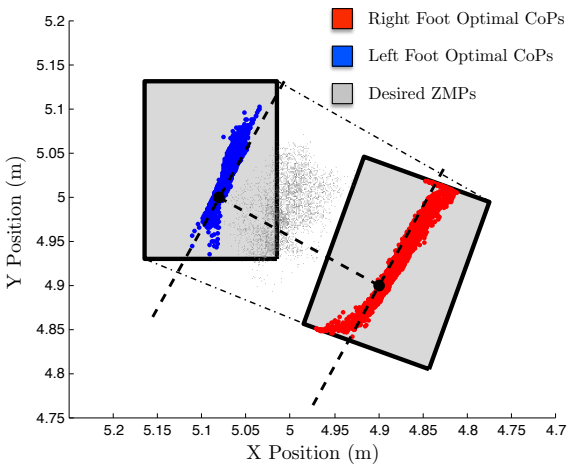

Figure 7: Optimal CoPs as found by the Contact Vertices (CV) force distribution algorithm for the CMU reaching motion.

4.4 Results

A solution method to the Contact Vertices (CV) formulation was again developed with KNITRO and was tested to solve the FDP for execution of the CMU reaching motion. The CV formulation was found to result in similar optimal CoPs as the Foot CoPs formulation, but the convexity of the CV formulation makes it applicable for use in real-time control. The optimal CoPs for the CV formulation are show in Fig. 7 and are predominantly found along the lines perpendicular to the line between the ankle centers. The solution algorithm is an interior-point algorithm and obtains convergence at all instances of the CMU reaching motion. A solution to the FDP was found in 1.75 ms on average, and in 10.8 ms in the worst case. Thus, on average, this method is over 40 times faster than the Foot CoPs algorithm.

Table 1 provides a comparison between the two formulations developed thus far. The nonlinear equality constraints and non-convex objective found in the Foot CoPs formulation are eliminated at the expense of extra variables in the CV formulation. The average computation times are given for the CMU reaching motion with square feet ($m = 8$). In both formulations, iterates were initialized to the previous optimal solution to improve convergence time.

5 Application to Uneven Terrain

While the results thus far have focused on force distribution for motions on even terrain, the formulations presented are general to any foot orientation and position. In fact, the feasibility of an instance of the FDP on uneven terrain provides a certificate of instantaneous dynamic feasibility in a manner that is analogous to the computed ZMP falling within the support polygon on even terrain. Thus feasibility of the FDP within our formulation provides an alternative check of dynamic feasibility to the conditions presented in other work.[19, 24, 27]

The CV formulation was used to optimize the force distribution for the CMU reaching motion on the end of a ramp. A snapshot from the motion in this setting is shown in Fig. 8(a). The uneven footholds demonstrate the generality of the formulation to handle different foot heights as well as orientations. Once again, a dynamically feasible desired motion was prescribed. The resultant optimal foot CoPs are shown in Fig. 8(b). The lines perpendicular to the line between the ankle centers are shown in this figure to compare the behavior of this solution to the simplified case. For the right foot, the perpendicular line is projected along the global z-axis to the local plane of contact. As long as the vector opposite gravity is within each friction cone around the contact normals, this simplified solution still has the potential to provide quick sub-optimal solutions. As expected, the solution to the FDP on uneven terrain experiences the same computational performance as on even terrain. For this motion, the CV solution algorithm was able to determine an optimal force distribution in 1.73 ms on average.

(a)

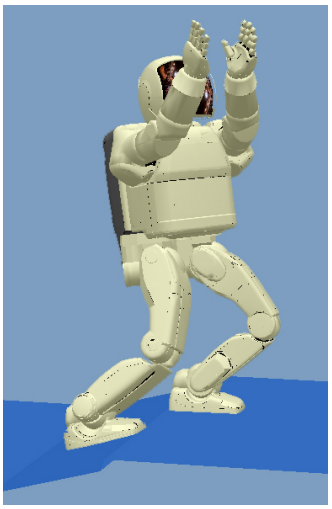

(b)

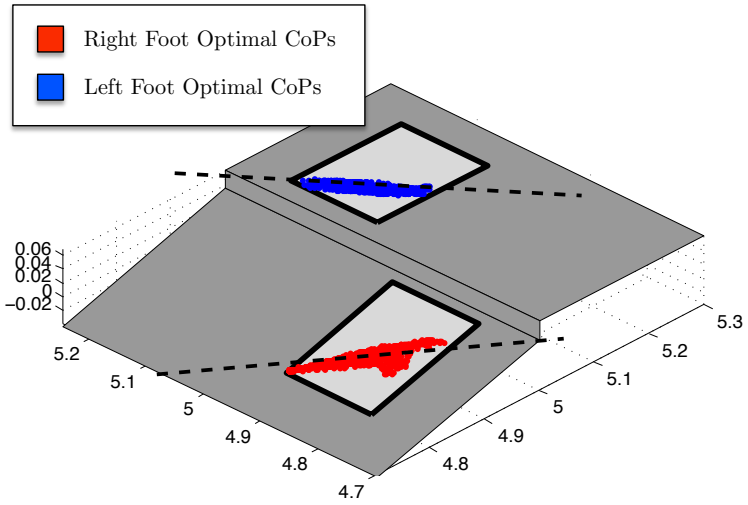

Figure 8: (a) Motion snapshot from the CMU reaching motion on the end of a ramp. The uneven foot positions highlight the generality of the formulation to handle feet at different heights and with different orientations. (b) Optimal local CoPs for the CMU reaching motion while standing on the end of a ramp. Optimal CoPs still follow the heuristic identified from the simplified formulation, with the lines perpendicular to the line between the ankle centers projected (along the z-axis) to the local plane of contact.

6 Alternative Objective: Foot Center of Pressure Margins

The ankle effort objective considered previously can be effective, yet it often places foot CoPs at extreme locations to obtain optimal torque-squared performance. This can be undesirable, as local CoPs near foot boundaries provide less margin for error against model or terrain uncertainties that can lead to foot roll. On the other hand, foot CoPs placed near the center of support can help to prevent unwanted transitions to edge or point contact in the case of contact disturbances.[15]

To address these issues, it is desirable to design a formulation which achieves near-optimal torque-squared performance yet prevents the local CoPs from being placed at the foot boundaries. This will be accomplished through an augmented objective and penalty approach that optimizes the foot CoP margins. Our approach more directly penalizes transitions to edge contacts as compared to previous approaches that penalize tangential moments at desired foot CoPs.[15,29]

6.1 Auxiliary Variables and Objective Augmentation

A number of auxiliary variables will be defined to assist in the foot CoP margin optimization. We note that the local CoP for foot i reaches the foot boundary when:

1. At least one of the contact vertices has zero associated force. That is, $f_{ij}^z = 0$, for some $j \in \{1, \ldots, m_i\}$. Still, this is not a *sufficient* condition for edge contact.

2. All of the load for a foot is placed on a single edge. This occurs when the total force for a foot resides at two adjacent vertices, that is $\sum_j f_{ij}^z = f_{ik}^z + f_{ik'}^z$ for some $k \in \{1, \ldots, m_i\}$ and some vertex k' adjacent to vertex k for foot i.

In this spirit, we make the following definitions. Define the *adjacency sets*:

$$\mathcal{A}_i := \{(k, k') \in \{1, \ldots, m_i\}^2 \,|\, \text{vertex } k \text{ is adjacent to } k'\}\,. \tag{19}$$

With these sets, for each foot we define the maximum edge force as:

$$\overline{F_i} = \max_{(k,k') \in \mathcal{A}_i} {}^i f_{ik}^z + {}^i f_{ik'}^z \tag{20}$$

and the total foot load as:

$$L_i = \sum_{j=1}^{m_i} {}^i f_{ij}^z \,.$$

We define the minimum vertex force as:

$$\underline{f_i} = \min_{j \in \{1,\ldots,m_i\}} {}^i f_{ij}^z \,. \tag{21}$$

Thus, the local foot CoP becomes undesirable as $\underline{f_i}$ approaches 0 and $\overline{F_i}$ approaches L_i. To penalize $\underline{f_i} \to 0$, the objective is augmented with a term:

$$\sum_{i=1}^{2} \rho_0 \exp(-r_0 \underline{f_i}) \tag{22}$$

which is convex in the auxiliary variable $\underline{f_i}$. This term assigns a fixed penalty ρ_0 when any contact vertex carries no load and decays at a rate controlled by r_0. Similarly a penalty is introduced on $\overline{F_i}$:

$$\sum_{i=1}^{2} \rho_1 L_i \exp\left[r_1 \left(\frac{\overline{F_i}}{L_i} - 1\right)\right]. \tag{23}$$

This term is convex, as it is a scalar multiple of a perspective function on the exponential function (and satisfies the restriction that $L_i \geq 0$). While initially only the penalty from (23) was used, the addition of the penalty in (22) led to more computational reliability in the algorithm's real-time convergence.

6.2 Formulation

These penalties will be added linearly to the previous objective to provide an opportunity to optimize torque performance without sacrificing CoP margins. Overall the modified CV formulation for indirect CoP optimization is:

$$\begin{aligned}
\min\ & \mathbf{f}_c^T \mathbf{Q} \mathbf{f}_c + \sum_i \rho_0 \exp(-r_0 \underline{f_i}) + \rho_1 L_i \exp\left[r_1 \left(\frac{\overline{F_i}}{L_i} - 1\right)\right] \\
\text{s.t. } & {}^0\mathbf{w} = \mathbf{A}\mathbf{f}_c \\
& \mathbf{f}_c \in \mathcal{K}_c \\
& L_i = \sum_j {}^i f_{ij}^z && \forall i \in \{1,2\} \\
& \overline{F_i} \geq {}^i f_{ik}^z + {}^i f_{ik'}^z && \forall i \in \{1,2\}, (k,k') \in \mathcal{A}_i \\
& \underline{f_i} \leq {}^i f_{ij}^z && \forall i \in \{1,2\}, j \in \{1,\ldots,m_i\}
\end{aligned}$$

While $\overline{F_i}$ and $\underline{f_i}$ are not explicitly constrained to be maxima and minima as in (20) and (21), any optimum will satisfy these equations. This is accomplished by the terms in the objective that seek to drive down $\overline{F_i}$ and drive up $\underline{f_i}$.

6.3 Performance and Parameter Selection

The selection of the parameters ρ_0, ρ_1, r_0, and r_1 have a substantial effect on the resultant optimal CoPs. While ρ_0 and ρ_1 control the trade-off between torque squared and foot CoP margin objectives, the rate terms r_0 and r_1 control how quickly the maximum penalties decay. That is, a very large value for r_1 will result in a penalty on CoPs that is heavily localized to the edge of the foot. To illustrate the role of this parameter, a number of parameter selections and the resultant optimal CoPs are shown in Fig. 9. As shown, the foot CoP margin optimization succeeds in improving the CoP locations over the original torque-squared objective alone. As the penalty decay rate is decreased, the optimal CoPs are pushed towards the center of foot support, at the expense of ankle effort. Still, the average ankle effort for the most extreme of these

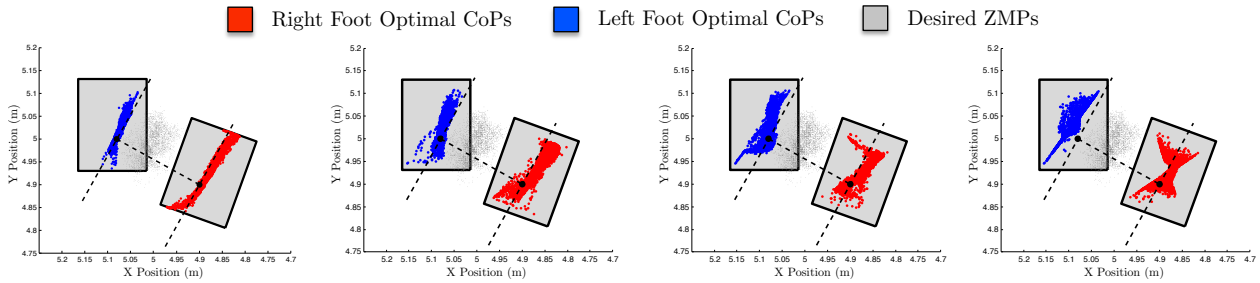

Figure 9: Optimal foot CoPs before and after foot CoP margin optimization. The last three cases employ foot CoP margin optimization with parameters $\rho_0 = 5000$ and $\rho_1 = 10$. Different selections of parameters r_0 and r_1 are employed, where r_1 is shown below each subfigure, and $r_0 = r_1/150$.

modifications (the $r_1 = 30$ case) is only about 25% more than the original case. All solutions obtain real-time convergence with average convergence time on the order of 3 - 6 ms for each of the cases.

Proper selection of the parameters ρ_0 and ρ_1 does depend on the system. They should be selected such that ρ_0 is approximately ρ_1 times larger than average foot load (approximately half the system's weight). These parameters then should be scaled proportionally until the desired tradeoff between objectives is reached.

7 Conclusions

This paper has presented and analyzed two general formulations of the force distribution problem for a humanoid robot that enable a unified treatment of joint torque and CoP objectives. While previous developments haven't explicitly enforced friction constraints or have used linear approximations to the friction cones, our work handles friction constraints more generally and considers a formulation to push foot CoPs away from foot boundaries. On level terrain, our Foot CoPs formulation enables sub-optimal solutions to the ankle effort minimization problem, that have been measured at a rate of over 1 MHz, through simplifications to the formulation. In contrast, our Contact Vertices (CV) formulation possesses convexity and enables solution of the FDP at over 100 Hz for even and uneven terrain. These computational rates are on par with a previous application of contact force optimization for real-time inverse dynamics.[10] As an immediate consequence, the CV formulation provides a computational approach to verify dynamic feasibility for motions on uneven terrain. Although the CV formulation explicitly optimizes a discrete set of contact forces, we have developed a novel FDP objective that allows optimization of foot CoPs to avoid foot roll through penalization of CoPs near foot boundaries.

This work has laid the foundation for high-level controllers to employ force distribution in a variety of contexts for force-controlled humanoids. These algorithms have provided the real-time capability needed for force distribution optimization and have the potential to enable humanoids to plan and perform compliant motions in increasingly complex contact conditions. Intelligently scheduling the objectives presented in this paper proves to be an interesting avenue for future investigation.

8 Acknowledgments

This work was supported in part by fellowships from the Ohio Space Grant Consortium, The National Science Foundation, and The Ohio State University. Other funding was provided by a research contract from the Honda Research Institute USA to The Ohio State University, and by Grant No. CNS-0960061 from the National Science Foundation with a subaward to The Ohio State University. Part of the data used in this project was obtained from mocap.cs.cmu.edu. The database was created with funding from NSF EIA-0196217.

References

[1] D. E. Orin and S. Y. Oh, Control of force distribution in robotic mechanisms containing closed kinematic chains, *J. Dynamic Syst. Meas. Contr.* **103**(2) (1981) 134–141.

[2] K. Waldron, Force and motion management in legged locomotion, *IEEE J. of Robotics and Automation* **2**(4) (1986) 214–220.

[3] C. A. Klein and S. Kittivatcharapong, Optimal force distribution for the legs of a walking machine with friction cone constraints, *IEEE Trans. on Robotics and Automation* **6**(1) (1990) 73–85.

[4] F.-T. Cheng and D. Orin, Optimal force distribution in multiple-chain robotic systems, *IEEE Trans. on Systems, Man and Cybernetics* **21**(1) (1991) 13–24.

[5] M. Mistry, J. Buchli, and S. Schaal, Inverse dynamics control of floating base systems using orthogonal decomposition, in *IEEE Int. Conf. on Robotics and Automation* (2010), pp. 3406–3412.

[6] G. Bin Hammam, D. Orin, and B. Dariush, Whole-body humanoid control from upper-body task specifications, in *IEEE Int. Conf. on Robotics and Automation* (2010), pp. 3398–3405.

[7] D. E. Orin and A. Goswami, Centroidal momentum matrix of a humanoid robot: Structure and properties, in *IEEE/RSJ Int. Conf. on Intelligent Robots and Systems* (2008), pp. 653–659.

[8] S.-H. Hyon, Compliant terrain adaptation for biped humanoids without measuring ground surface and contact forces, *IEEE Trans. on Robotics* **25**(1) (2009) 171–178.

[9] S.-H. Lee and A. Goswami, A momentum-based balance controller for humanoid robots on non-level and non-stationary ground, *Autonomous Robots* **33**(4) (2012) 399–414.

[10] L. Righetti, J. Buchli, M. Mistry, and S. Schaal, Control of legged robots with optimal distribution of contact forces, in *IEEE-RAS Int. Conf. on Humanoid Robots* (2011), pp. 318–324.

[11] S.-H. Hyon, J. Hale, and G. Cheng, Full-body compliant human humanoid interaction: Balancing in the presence of unknown external forces, *IEEE Trans. on Robotics* **23**(5) (2007) 884–898.

[12] B. J. Stephens and C. G. Atkeson, Dynamic balance force control for compliant humanoid robots, in *IEEE/RSJ Int. Conf. on Intelligent Robots and Systems* (2010), pp. 1248–1255.

[13] B.-K. Cho, S.-S. Park, and J.-H. Oh, Controllers for running in the humanoid robot, HUBO, in *Proc. of the IEEE Int. Conf. on Humanoid Robots* (2009), pp. 385–390.

[14] K. Harada, S. Kajita, H. Saito, M. Morisawa, F. Kanehiro, K. Fujiwara, K. Kaneko, and H. Hirukawa, A humanoid robot carrying a heavy object, in *IEEE Int. Conf. on Robotics and Automation* (2005), pp. 1712–1717.

[15] L. Sentis, J. Park, and O. Khatib, Compliant control of multicontact and center-of-mass behaviors in humanoid robots, *IEEE Trans. on Robotics* **26**(3) (2010) 483–501.

[16] S. Kajita, F. Kanehiro, K. Kaneko, K. Fujiwara, K. Harada, K. Yokoi, and H. Hirukawa, Biped walking pattern generation by using preview control of Zero-Moment Point, in *Proceedings of the IEEE International Conference on Robotics and Automation (ICRA)* (2003), pp. 1620–1626.

[17] L. Sentis and O. Khatib, Synthesis of whole-body behaviors through hierarchical control of behavioral primitives, *Int. Journal of Humanoid Robotics* **2**(4) (2005) 505–518.

[18] L. Righetti, M. Mistry, J. Buchli, and S. Schaal, Inverse dynamics control of floating-base robots with external contraints: a unified view, in *IEEE Int. Conf. on Robotics and Automation* (2011), pp. 1085–1090.

[19] Y. Zheng and C.-M. Chew, Fast equilibrium test and force distribution for multicontact robotic systems, *J. of Mechanisms and Robotics* **2**(2) (2010) 021001:1–11.

[20] R. Featherstone and D. Orin, Chapter 2: Dynamics, in *Springer Handbook of Robotics*, B. Siciliano and O. Khatib (eds.), (Springer, New York, 2008).

[21] J. Kerr and B. Roth, Analysis of multifingered hands, *The International Journal of Robotics Research* **4**(4) (1986) 3–17.

[22] S. Boyd and L. Vandenberghe, *Convex Optimization*, (Cambridge Univ. Press, Cambridge, U.K., 2004).

[23] L. M. Nashner, Sensory, neuromuscular, and biomechanical contributions to human balance, in *American Physical Therapy Association (APTA) Forum* (1989), pp. 5–12.

[24] S. Takao, Y. Yokokohji, and T. Yoshikawa, FSW (feasible solution of wrench) for multi-legged robots, in *IEEE Int. Conf. on Robotics and Automation* (2003), pp. 3815–3820.

[25] A. Zaslavski, R. Byrd, J. Nocedal, and R. Waltz, KNITRO: An integrated package for nonlinear optimization, in *Large-Scale Nonlinear Optimization*, P. Pardalos, G. Pillo, and M. Roma (eds.), (Springer US, New York, NY, 2006), pp. 35–59.

[26] Carnegie Mellon University, CMU graphics lab motion capture database, Internet page (http://mocap.cs.cmu.edu), jump up to grab, reach for, tiptoe motion.

[27] H. Hirukawa, S. Hattori, K. Harada, S. Kajita, K. Kaneko, F. Kanehiro, K. Fujiwara, and M. Morisawa, A universal stability criterion of the foot contact of legged robots - adios ZMP, in *IEEE Int. Conf. on Robotics and Automation* (2006), pp. 1976–1983.

[28] S. Boyd and B. Wegbreit, Fast computation of optimal contact forces, *IEEE Transactions on Robotics* **23**(6) (2007) 1117–1132.

[29] K. Yamane and J. Hodgins, Control-aware mapping of human motion data with stepping for humanoid robots, in *Proc. of the IEEE/RSJ Int. Conf. on Intelligent Robots and Systems* (2010), pp. 726–733.